physica status solidi pss c
www.pss-c.com
current topics in solid state physics

Pauli blockade transport in the cotunneling regime through a double quantum dot

H.W. Liu[1,2,3], **T. Fujisawa**[1,4], **T. Hayashi**[1], and **Y. Hirayama**[1,2]

[1] NTT Basic Research Laboratories, NTT Corporation, 3-1 Morinosato-Wakamiya, Atsugi 243-0198, Japan
[2] SORST-JST, 4-1-8 Honmachi, Kawaguchi, Saitama 331-0012, Japan
[3] National Laboratory of Superhard Materials, Institute of Atomic and Molecular Physics, Jilin University, Changchun 130012, P.R. China
[4] Tokyo Institute of Technology, 2-12-1 Ookayama, Meguro-ku, Tokyo 152-8551, Japan

Received 1 May 2006, accepted 14 June 2006
Published online 24 November 2006

PACS 71.70.Gm, 73.23.Hk, 73.40.Gk, 73.63.Kv

Pauli spin blockade in the cotunneling transport through an effective two-electron double quantum dot (™10 electrons in each dot) has been presented. In the cotunneling regime where the two-electron (1,1) and (0,2) states (ordered pairs denote the effective electron numbers in each dot) are far below the Fermi energy of the leads, we can concentrate on the two-electron tunnelling transitions and detect singlet-triplet splitting arising from the exchange interaction between the two electron spins with improved resolution. We discuss the cotunneling transport by considering the coherent and incoherent coupling between the dots in connection with the singlet-triplet splitting.

phys. stat. sol. (c) **3**, No. 11, 3766 – 3769 (2006) / **DOI** 10.1002/pssc.200671532

WILEY-VCH

phys. stat. sol. (c) **3**, No. 11, 3766–3769 (2006) / **DOI** 10.1002/pssc.200671532

Pauli blockade transport in the cotunneling regime through a double quantum dot

H.W. Liu[*,1,2,3], **T. Fujisawa**[1,4], **T. Hayashi**[1], and **Y. Hirayama**[1,2]

[1] NTT Basic Research Laboratories, NTT Corporation, 3-1 Morinosato-Wakamiya, Atsugi 243-0198, Japan
[2] SORST-JST, 4-1-8 Honmachi, Kawaguchi, Saitama 331-0012, Japan
[3] National Laboratory of Superhard Materials, Institute of Atomic and Molecular Physics, Jilin University, Changchun 130012, P.R. China
[4] Tokyo Institute of Technology, 2-12-1 Ookayama, Meguro-ku, Tokyo 152-8551, Japan

Received 1 May 2006, accepted 14 June 2006
Published online 24 November 2006

PACS 71.70.Gm, 73.23.Hk, 73.40.Gk, 73.63.Kv

Pauli spin blockade in the cotunneling transport through an effective two-electron double quantum dot (™10 electrons in each dot) has been presented. In the cotunneling regime where the two-electron (1,1) and (0,2) states (ordered pairs denote the effective electron numbers in each dot) are far below the Fermi energy of the leads, we can concentrate on the two-electron tunnelling transitions and detect singlet-triplet splitting arising from the exchange interaction between the two electron spins with improved resolution. We discuss the cotunneling transport by considering the coherent and incoherent coupling between the dots in connection with the singlet-triplet splitting.

1 Introduction Two-electron double quantum dot (DQD) is a superb system for studying fundamental spin physics. Singlet-triplet (ST) splitting appears originating from the exchange interaction between the two electron spins. The ingress of a single electron to the dots is determined not only by Coulomb repulsion but also by spin correlation. Spin correlation leads to a Pauli spin blockade, at which the transport is blocked when the two electrons have a spin triplet correlation [1]. More recently, a Pauli spin blockade with nealry degenerated ST splitting has been extensively employed for detecting and taming the nuclear spins in the host crystal [2–4]. This kind of spin-selective tunneling is not limited to the two-electron DQD and may occur generally in a DQD with more than two electrons. Here we present the Pauli spin blockade in an effective DQD containing around 10 electrons in each dot. We focus on the blockade transport in a cotunneling regime where the ST splitting can be detected sensitively due to a reduced lifetime broadening of the tunneling resonance peak [5]. A clear current rectification with negative differential conductance (NDC) is observed and discussed by considering the coherent and incoherent interdot coupling in connection with the ST splitting. These discussions are expected to reveal transitions from incoherent tunneling to coherent tunneling with an increase in the ST splitting, which is quite important for swapping spin information in a quantum computing achitecture.

2 Experimental Gate-defined double dots are fabricated using a patterned AlGaAs/GaAs heterostructure [inset to Fig. 1(a)]. The tunneling rate $\gamma_L(\gamma_R)$ of the left (right) barrier separating the left (right) dot and the source (drain) electrode as well as the interdot coupling t_c of the central barrier are controlled by gate voltages $V_{GL(R)}$ and V_{GC}, respectively. All experiments were performed by dc current measurement at zero magnetic field (unless noted otherwise) at an electron temperature of $T_e \sim 25$ mK

* Corresponding author: e-mail: liuhw@will.brl.ntt.co.jp, Phone: +81 46 240 3181, Fax: +81 46 240 4727

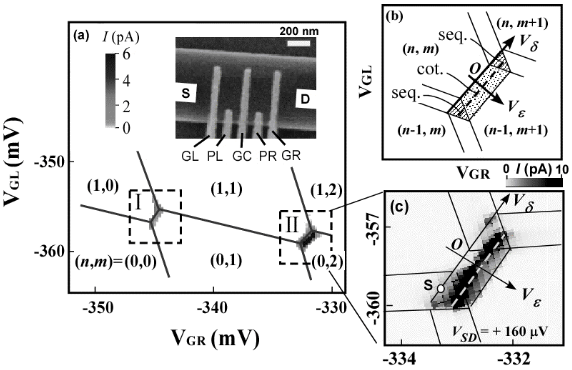

Fig. 1 (a) Dependence of current I on gate voltages V_{GL} and V_{GR} The ordered pairs denote the effective electron numbers in each dot. Solid lines are guides for eyes. Inset shows an SEM image of our DQD. (b) Schematic charge diagram in the V_{GL}-V_{GR} plane. Sequential and charge-conserved cotunneling regions are denoted by hatched and dotted patterns, respectively. Dashed line denotes a resonant tunneling related to the excited state. (c) Current peak in the region II (a) at $V_{SD} = +160\ \mu V$, which is comparable to (b). Point S is traced on the resonant line along V_δ in the sequential regime.

determined from Coulomb peak width of a single dot. Figure 1(a) shows current I through the dots as a function of V_{GL} and V_{GR}, changing the equilibrium electron numbers (n, m) in the left and right dots, respectively [6]. By applying more negative V_{GL} and V_{GR} (expelling the electrons in each dot), the last two current peaks are resolved in regions I and II. Each dot there might contain about 10 electrons roughly estimated from the average level spacing in a single dot. However, the labeled *effective* electron numbers n and m in the range from 0 to 2 explain experiments well. A schematic diagram of the current peak spreading out in the V_{GL}-V_{GR} plane at a finite source-drain bias V_{SD} is drawn in Fig. 1(b). Sequential tunneling (dot levels are located within the bias window) and charge-conserved cotunneling regions are identified by hatched and dotted patterns, respectively. Two sweeping voltages V_δ and V_ε are introduced: Changing V_δ shifts the average electrochemical potential δ of the (n, m) and (n-1, m+1) charge states; Changing V_ε gives the energy difference ε between the two states. The origin O ($V_\delta = V_\varepsilon = 0$, $\delta = \varepsilon = 0$) is taken on the solid line along V_δ [representing a resonant tunneling between the (n, m) and (n-1, m+1) ground states] in the middle of the N(=n+m)-electron Coulomb blockade region. The dashed line denotes a resonant tunneling related to the (n, m) and (n-1, m+1) excited states. This diagram is presented experimentally by the magnified plot in region II [Fig. 1(c)]. It is clearly shown, at positive bias, that the resonant tunneling through the ground states is suppressed and thereby shows weak current except for the two outermost edges in the sequential tunneling regions. However, the resonant transport related to the excited states is allowed and shows strong tunneling current. At negative bias, both resonant tunneling lines are observed (data not shown). Sweeping V_{SD} at the point S on V_δ in the sequential regime, the I-V_{SD} curve featuring a current rectification is plotted by hollow circles in Fig. 2(a). In addition, the energy spacing between the two resonant lines decreases with increasing magnetic field B (perpendicular to

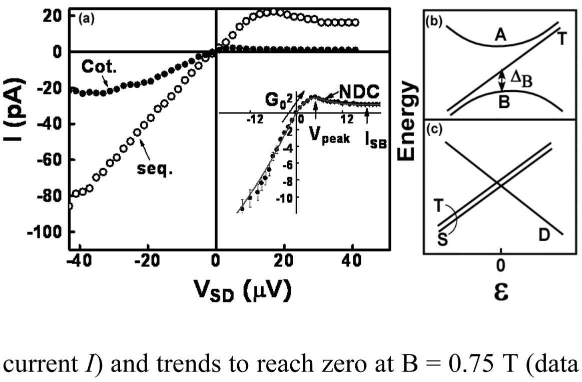

Fig. 2 (a) I-V_{SD} curve traced at point S (hollow circles) and origin O (solid circles) in Fig.1(c). The magnified plot at the origin is shown in inset, where the grey line is calculated by the second model we proposed. (b) Anti-crossing diagram for two-electron DQD with coherent interdot coupling. Bonding and antibonding bands are denoted by B and A, respectively. T represents the (1,1) triplet state. Δ_B corresponds to the ST splitting. (c) Schematic energy diagram of DQD with incoherent interdot coupling. A degenerated ST splitting is assumed in this case.

current I) and trends to reach zero at B = 0.75 T (data not shown). All data as mentioned above resemble the reported Pauli spin blockade in the sequential transport through a true two-electron DQD. Therefore, it is reasonable that the current peak in the region II in our case denotes a tunneling transition between *effective* two-electron (1,1) and (0,2) states, at which the Pauli spin blockade is clearly demonstrated. Furthermore, this blockade effect is not observed in the neighbor region I because the current peak there corresponds to *effective* one-electron transport.

In the cotunneling regime, similar bias-polarity current I (traced at the origin O) induced by the Pauli spin blockade is plotted by solid circles in Fig. 2(a). Different from the current rectification in the sequential tunneling transport (first-order process), that in the cotunneling regime shows a very tiny peak with small saturated current [see the magnified plot in the inset to Fig. 2(a)]. Therein we can focus on the two-electron tunnelling transitions and detect the ST splitting with improved resolution due to a reduced lifetime broadening of the tunneling resonance in the high-order cotunneling transport. Figure 3 summarizes the zero-bias conductance G_0, the spin blockade current I_{SB} at V_{SD} = 50 μV, and the current peak position V_{peak} as a function of ε and δ. In order to avoid the sequential tunneling effect, the cotunneling region is confined to the δ range of -90 to 90 μeV [7]. We fit G_0, I_{SB} and V_{peak} with two simple models, one of which takes coherent interdot coupling and the other incoherent interdot coupling into account.

3 Discussion In the first model, we consider the coherent coupling between the dots but neglecting decoherence, spin-orbit interaction and thermal effect. Coherent coupling between the (1,1) and (0,2) singlet states induces a bonding (B) and antibonding (A) splitting [Fig. 2(b)]. At small bias [$eV_{SD} < \Delta_B$, Δ_B is the energy spacing between the bonding and triplet (T) states], elastic cotunneling through the bonding state mainly contributes to the linear conductance. In the spin blockade region at large V_{SD}, I_{SB} is approximately determined by the lifetime of the (1,1) triplet state which depends on a spin relaxation via inelastic cotunneling from the T to B states. G_0 and I_{SB} are given by [8]

$$G_0 = \frac{e^2}{h}\hbar^2\gamma_e^2 V^{-2}\frac{(\hbar t_c)^2}{\varepsilon^2 + 4(\hbar t_c)^2}\ , \tag{1}$$

$$I_{SB} = \frac{e}{h}\hbar^2\gamma_s^2 V^{-2}\frac{(\hbar t_c)^2}{\sqrt{\varepsilon^2 + 4(\hbar t_c)^2}}, \tag{2}$$

where $V^{-1} = (U/2+\delta)^{-1} + (U/2-\delta)^{-1}$ and U (= 255 μeV) is the electrostatic coupling energy [7]. γ_e is defined as the effective tunneling rate for elastic cotunneling involving higher-order tunneling processes (e.g., Kondo effect), and can be simplified to $\gamma_e = \sqrt{\gamma_L\gamma_R}$ by only considering the second-order tunneling. γ_s is the effective tunneling rate for spin-flip inelastic cotunneling ($\gamma_s \equiv \gamma_L = \gamma_R$ is assumed for simplifying the expression). A current peak with NDC appears when the linear current at the onset of the spin blockade is higher than the blockade current ($G_0V_{peak} > I_{SB}$). Based on Eqs. (1) and (2), the peak is expected at $\gamma_e > \gamma_s$. Second-order cotunneling with a strong asymmetric barrier and higher-order tunneling processes ensures $\gamma_e >> \gamma_s$ in our case. When the current peak is well defined, we can relate V_{peak} to Δ_B, $eV_{peak} = \Delta_B = \frac{1}{2}(\sqrt{\varepsilon^2 + 4(\hbar t_c)^2} + \varepsilon)$ [7].

In the second model, we discuss the peak by considering the thermal effect but neglecting coherent coupling (a classical model with zero ST splitting). The degenerated (1,1) singlet (S) and triplet (T) states cross with the (0,2) singlet state (D) at ε = 0, as schematically shown in Fig. 2(c). In addition, we take phonon-related inelastic tunneling between the S and D states into account [9]. Assume the inelastic tunneling rate is much larger than the cotunneling rate between the S (or T) and D states and both are larger than the spin exchange rate between the S and T states, which ensures the appearance of a clear peak with NDC [7]. G_0 and I_{SB} are derived from the cotunneling current I_{cot} by solving the rate equations related to all transitions mentioned above,

$$G_0 = \frac{e^2}{4h}\hbar^2\gamma_e^2 V^{-2}\frac{12\varepsilon}{kT(1+e^{\varepsilon/k_BT_e} - 2e^{-\varepsilon/k_BT_e})}, \tag{3}$$

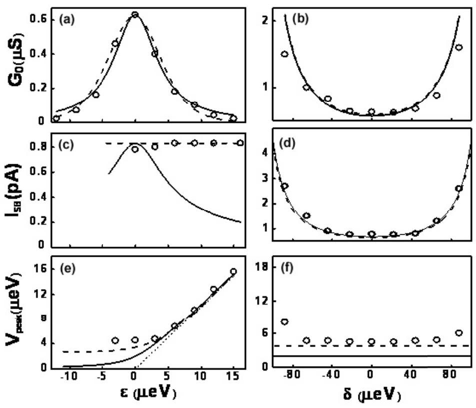

Fig. 3 Zero-bias conductance G_0 (a) and (b), spin blockade current I_{SB} (c) and (d) at V_{SD} = 50 µV and current peak position V_{peak} (e) and (f) as a function of ε and δ. Note that (a), (c) and (e) are obtained at δ = 0 and (b), (d) and (f) are for ε = 0. Solid curves are calculated by the equations in the first model with parameters $\hbar t_c = 2\mu eV$, $\hbar\gamma_e = 16.2\mu eV$, and $\hbar\gamma_s = 9.3\mu eV$. Dashed lines were plotted based on the second model with $\hbar\gamma_e = 7.9\mu eV$, $\hbar\gamma_s = 6.2\mu eV$, and $k_B T_e = 2.2\mu eV$. The dotted line in (e) is a reference for $eV_{peak} = \varepsilon$.

$$I_{SB} = \frac{e}{h}(\hbar\gamma_s)^2 V^{-2} k_B T_e, \tag{4}$$

where k_B is Boltzmann's constant. V_{peak} corresponds to the V_{SD} value satisfying $dI_{cot}/dV_{SD} = 0$.

The solid and dashed curves in Fig. 3 are calculated by the first and second model, respectively. It is clearly shown that the second model fits the data well [also see the fitting curve in the inset of Fig. 2(a)]. In fact, we should note that the fitting parameter $\hbar t_c = 2\mu eV$ in the first model near the thermal energy $k_B T_e$ (= 2.2 µeV), which does not satisfy our assumption. Thus, the current peak with NDC in the case of weak interdot coupling t_c is induced by the thermal effect.

4 Conclusions We demonstrated Pauli spin blockade in a DQD with more than two electrons. In the cotunneling regime, we focused on the blockade transport and observed the current rectification with NDC. Two simple models, one of which takes coherent interdot coupling and the other incoherent interdot coupling into account, were employed for fitting the data. The incoherent model seems to explain experiments well. Nevertheless, it is believed that the coherent model can be effectively applied to detect ST splitting with increasing the interdot coupling t_c. Systematic analyses by the two models should reveal transitions from incoherent tunneling to coherent tunneling in connection with the ST splitting.

Acknowledgements We thank K. Ono and Y. Tokura for useful discussions. This work was partly supported by Strategic Information and Communications R&D Promotion Program (SCOPE) from the Ministry of Internal Affairs and Communications of Japan, and by Grant-in-Aid for Scientific Research from the Japan Society for the Promotion of Science.

References

[1] K. Ono, D. G. Austing, Y. Tokura, and S. Tarucha, Science **297**, 1313 (2002).
[2] A. C. Johnson, J. R. Petta, J. M. Taylor, A. Yacoby, M. D. Lukin, C. M. Marcus, M. P. Hanson, and A. C. Gossard, Nature (London) **435**, 925 (2005).
[3] J. R. Petta, A. C. Johnson, J. M. Taylor, E. A. Laird, A. Yacoby, M. D. Lukin, C. M. Marcus, M. P. Hanson, and A. C. Gossard, Science **309**, 2180 (2005).
[4] F. H. L. Koppens, J. A. Folk, J. M. Elzerman, R. Hanson, L. H. Willems van Beveren, I. T. Vink, H. P. Tranitz, W. Wegscheider, L. P. Kouwenhoven, and L. M. K. Vandersyphen, Science **309**, 1346 (2005).
[5] S. De Franceschi, S. Sasaki, J. M. Elzerman, W. G. van der Wiel, S. Tarucha, and L. P. Kouwenhoven, Phys. Rev. Lett. **86**, 878 (2001).
[6] W. G. van der Wiel, S. De Franceschi, J. M. Elzerman, T. Fujisawa, S. Tarucha, and L. P. Kouwenhoven, Rev. Mod. Phys. **75,** 1(2003).
[7] H. W. Liu, T. Fujisawa, T. Hayashi, and Y. Hirayama, Phys. Rev. B **72**, 161305 (2005).
[8] M. Eto, Jpn. J. Appl. Phys. **40**, 1929 (2001).
[9] T. Fujisawa, D. G. Austing, Y. Tokura, Y. Hirayama, and S. Tarucha, Nature (London) **419**, 278 (2002).

